Reference to published article:
Nesbitt, J.A. & Lindsay, M.B.J. (2017). Vanadium geochemistry of oil sands fluid petroleum coke. *Environmental Science and Technology*, 51: 3102–3109. https://doi.org/10.1021/acs.est.6b05682

Vanadium Geochemistry of Oil Sands Fluid Petroleum Coke

Jake A. Nesbitt and Matthew B.J. Lindsay[*]

Department of Geological Sciences, University of Saskatchewan, Saskatoon, Saskatchewan, S7N 5E2, Canada

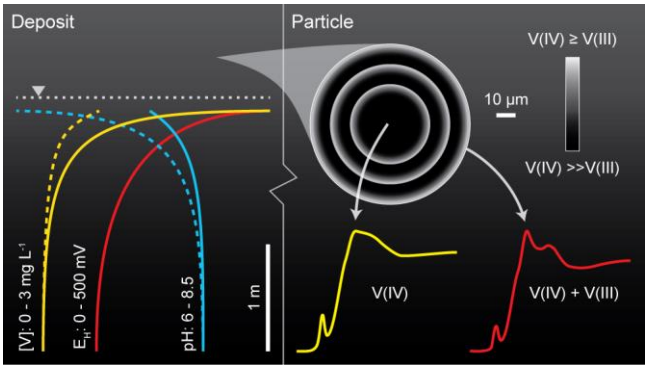

TOC/Abstract Art.

ABSTRACT

Vanadium has previously been linked to elevated toxicity of leachates derived from oil sands petroleum coke. However, geochemical controls on V mobility within coke deposits remain poorly constrained. Detailed examinations of pore-water and solid-phase V geochemistry were, therefore, performed on oil sands fluid petroleum coke deposits in Alberta, Canada. Sample collection focused on both active and reclaimed deposits, which contained more than 3×10^7 m^3 of fluid petroleum coke. Dissolved V concentrations were highest (up to 3.0 mg L^{-1}) immediately below the water table, but decreased rapidly with increasing depth. This trend corresponded to a transition from mildly acidic (pH 6 – 7) and oxic conditions to mildly alkaline (pH 7 – 8.5) and anoxic conditions. Scanning electron microscopy (SEM), electron microprobe analysis (EMPA) and micro-X-ray fluorescence (μXRF) mapping revealed coke particles exhibited an internal structure characterized by successive concentric layers. The outer margins of these layers were characterized by elevated V, Fe, Si, and Al concentrations, indicating the presence of inorganic phases. Micro-X-ray absorption near-edge structure (μXANES) spectroscopy revealed that V speciation was dominated by V(IV) porphyrins except at outer margins of layers, where octahedrally-coordinated V(III) was a major component. Minor to trace V(V) was also detected within fluid petroleum coke particles.

INTRODUCTION

Large quantities of petroleum coke are generated during upgrading of oil sands bitumen to synthetic crude oil. This carbonaceous material exhibits elevated S and trace element contents,[1] making it largely unsuitable for combustion or industrial applications. Consequently, greater than 10^8 t of petroleum coke is currently stockpiled in the Athabasca Oil Sands Region

(AOSR) of northern Alberta, Canada.[2] Mine closure landscapes could contain more than ten times this amount upon conclusion of mining.[3] Although petroleum coke offers utility as a construction material for mine closure landscapes, previous studies have reported toxic effects on invertebrates[4-6] and plants.[7] Baker et al.[8] observed increased V uptake by a macrophytic green alga and benthic invertebrates in coke-amended sediment from a reclamation wetland. Puttaswamy et al.[5] found that coke leachates were toxic to an aquatic invertebrate, and identified dissolved V as a principal source of this toxicity. Aeolian transport of fine particles from sub-aerial stockpiles has led to more widespread distribution in the AOSR.[9] Additionally, large stockpiles of oil sands petroleum coke have also been reported in urban industrial areas in major U.S. cities.[10] Consequently, a detailed understanding of V sources and mobility is critical for assessing and mitigating long-term environmental risk associated with this oil sands bitumen upgrading byproduct.

Vanadium occurs naturally at elevated concentration in oil sands bitumen and other heavy oil deposits.[11,12] Petroleum coke, generated during thermal conversion of the non-distillable bitumen fraction into volatile compounds, becomes enriched in trace elements present in heavy oils. Fluid petroleum coke from the AOSR typically exhibits total V concentrations of 1000 to 2000 mg kg^{-1}.[1,12-16] The V speciation of petroleum coke is dominated by V(IV) as the vanadyl ion (VO^{2+}) in porphyrin-like atomic coordination environments within asphaltenic micelles.[17,18] These stable metalloporphyrin complexes are generally resistant to both weathering and thermal decomposition.[12] Substantial V(IV) porphyrin breakdown during natural weathering has, however, been observed in Early Toarcian Age (183 Ma) black shales.[19] Additionally, thermal decomposition of these stable complexes has been reported at temperatures exceeding 400°C, [12] which is consistent with fluid coking temperatures of 480 to 565°C used during oil

sands bitumen upgrading.[20] Thermal decomposition of V porphyrins was previously inferred based on crystalline V-bearing nanocluster occurrence in AOSR fluid petroleum coke.[12] Vanadium was associated with Si, O, S and Fe within these nanoclusters; however, V speciation within this phase remains unknown.

Despite the apparent stability of V(IV) porphyrins, total dissolved V concentrations exceeding 2 mg L^{-1} for coke pore water and leachate have been reported.[4] Vanadium mobility within surface water and groundwater is strongly influenced by reduction-oxidation (redox), precipitation-dissolution, and sorption-desorption reactions.[21-24] Enhanced V leaching has been observed under oxic conditions at neutral to alkaline pH.[5,25] This transition metal exhibits six possible oxidation states, but V(III), V(IV) and V(V) dominate in the environment.[24,26] Although both V(IV) and V(V) can occur in petroleum coke leachates, V(IV) is rapidly oxidized to V(V) under oxic conditions.[27] Microbial reduction of dissolved V(V) to V(IV) and V(III) under anoxic conditions is also possible.[28] Aqueous V(V) speciation is generally dominated by $H_2VO_4^-$ and HVO_4^{2-} oxyanions at pH 4 to 10. Cationic V(III) and V(IV) species can occur under these conditions; however, precipitation of V (hydr)oxide phases can occur at elevated V(III) and V(IV) concentrations.[24] Redox processes, therefore, influence pH-dependent sorption-desorption and precipitation-dissolution reactions that control V mobility.[21] Consequently, complex interactions between (bio)geochemical processes likely control the occurrence and distribution of dissolved V within coke deposits.

This study focused on improving understanding of V geochemistry in oil sands fluid petroleum coke deposits. Detailed groundwater sampling was performed to constrain geochemical controls on V concentrations and distribution in active and reclaimed fluid coke deposits in the AOSR. Solid-phase analyses were performed to examine micro-scale V

speciation variability and potential pore-water V sources. Results improve capacity for predicting V mobility in oil sands mine closure landscapes and, more generally, provide new insight into environmental V geochemistry.

MATERIALS AND METHODS

Study Site. Field sampling was focused on fluid petroleum coke deposits at the Mildred Lake oil sands mine, which is located approximately 35 km north of Fort McMurray, Alberta, Canada (Figure 1). The two deposits examined during this study, Coke Beach (CB) and Coke Watershed (CW), are located within the containment dam for the Mildred Lake Settling Basin (MLSB). This active tailings pond contains fluid fine tailings (FFT), produced during bitumen extraction and upgrading, stored under a shallow water cover comprised of oil sands process water (OSPW).[29] The CB and CW deposits contain approximately 3×10^7 m^3 of fluid petroleum coke that was hydraulically deposited at the western margin of MLSB beginning in 2000. Coke Beach is a 1.5 km^2 sub-aerial deposit (i.e., coke is directly exposed to the atmosphere) where freshly-produced coke has been deposited since 2000. Coke Watershed is an inactive 0.28 km^2 deposit that received fresh coke from 2000 to 2003, when deposition ceased and an experimental reclamation soil cover was applied. The CB and CW deposits are hydraulically connected to FFT and the overlying OSPW water cover within MLSB.

Well Installations. Multi-level groundwater wells were installed at several locations in the CB (n = 5) and CW (n = 3) deposits (Figure 1) to assess spatial variability of V geochemistry. These wells were constructed from 0.3 cm inner diameter (ID) polyethylene (PE) tubes, which were perforated and screened over the bottom 10 cm with 125 µm Nitex mesh. Nine tubes were then fastened to a central 1.9 cm ID PE with screens spaced on center at 0.25 to

1.00 m intervals. The bundles were installed using a sonic drilling rig (ML SRS, Fraste S.p.A., Italy) by advancing 7.6 cm diameter steel casing fitted with an aluminum knock-out tip to 6.0 or 8.0 m below surface. Bundles were then lowered into the casing, which was then retrieved leaving the multi-level well and knock-out tip in place. Water was added to minimize the buoyancy of the well bundle during well installation. The water table was positioned 0.6 to 1.6 m below ground surface at CB well locations and 2.9 to 4.5 m below ground surface at CW well locations.

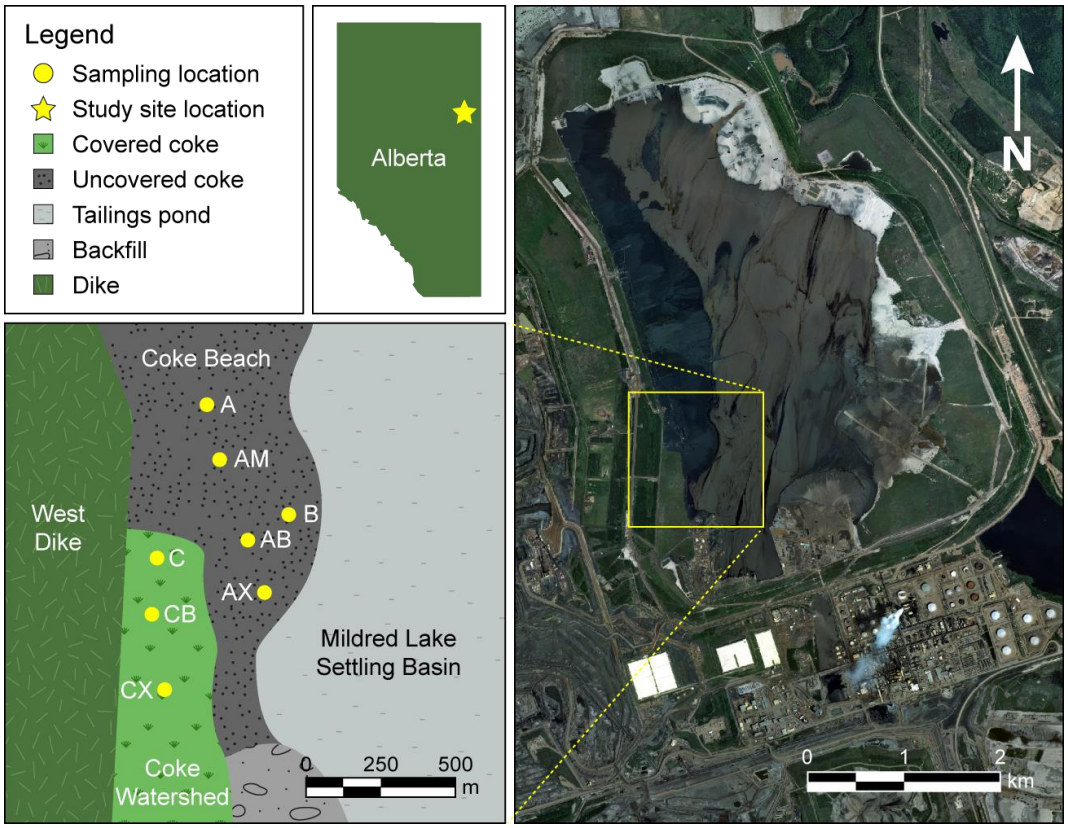

Figure 1. Plan view image of field site showing location in Alberta, Canada, aerial photo of the Mildred Lake Settling Basin, and plan view map of well installation and associated coring locations in the Coke Beach (CB) and Coke Watershed (CW) deposits.

Water Sampling and Analyses. Water samples were collected a minimum of 30 days after well installations. Static water table elevations were measured and three well volumes then were purged before sampling. A peristaltic pump (Geopump Series II, Geotech Environmental

Equipment Inc.) was connected with Pt-cured silicone pump tubing directly to the screened 0.3 cm ID tubing. The opposite end of the pump tubing was connected to an in-line flow-through cell, where measurements of pH, redox potential (Eh), electrical conductivity (EC), and temperature were performed. The pH electrode (Orion 8156BNUWP ROSS Ultra, Thermo Scientific, USA) was calibrated to NIST-traceable pH 7, 4 and 10 buffer solutions. The calibration was checked before each measurement and recalibration was completed as required. ZoBell's solution[30] and Light's solution[31] were used to verify Eh electrode (Orion 9678BNWP, Thermo Scientific, USA) performance. The conductivity cell (Orion 013010MD, Thermo Scientific, USA) was calibrated to NIST-traceable conductivity standards. Additional field measurements were performed, following removal of the flow-through cell, on water passed through inline 0.45 μm surfactant free cellulose acetate (SFCA) filters. Alkalinity was quantified by titration with H_2SO_4 to the bromocresol green methyl red endpoint (i.e., 4.5). Spectrophotometric NH_3-N and $H_2S_{(aq)}$ determinations were performed using salicylate (HACH Method 10031) and methylene blue (HACH Method 8131) methods, respectively.

Water samples for inorganic anion, dissolved organic carbon (DOC), and stable isotopes of water analyses were passed through 0.45 μm SFCA filters into PE bottles and stored at 4°C until analysis. Inorganic anions (Br, Cl, F, NO_3, NO_2, PO_4, SO_4) were quantified by ion chromatography (IC), while $\delta^{18}O$ and $\delta^{2}H$ vales were determined by cavity ring-down spectroscopy (L2120-i Isotopic Water Analyzer, Picarro, USA).[32] Samples for DOC analysis were transferred into amber borosilicate vials and acidified with 5% (v/v) H_3PO_4 remove inorganic carbon. Quantification was performed by wet UV/persulfate oxidation of DOC and thermal conductivity detection of evolved CO_2 (Model 1010 TOC Analyzer, OI Analytical, USA). Water samples for trace element and major cation analyses were passed through 0.1 μm

polyethersulfone membranes, acidified to < pH 2 using concentrated trace metals grade nitric acid (OmniTrace, EMD Millipore, USA), and stored in PE bottles at 4°C until analysis. Trace elements were quantified using inductively-coupled plasma mass spectrometry (ICP-MS; NexION 300D, Perkin Elmer, USA) and major cation concentrations were determined by inductively-coupled plasma optical emission spectrometry (ICP-OES; Varian Vista RL, Agilent Technologies, USA). Thermodynamic modelling of pore-water geochemistry was performed using PHREEQCi (Version 3.1.5)[33] with the MINTEQA2 V4 database.

Core Sampling and Analyses. Continuous core sampling was at locations in the CB (n = 5) and CW (n = 3) deposits corresponding to multi-level well installations (Figure 1). Core tubing was advanced in 2.0 m depth intervals using a sonic drilling rig (ML SRS, Fraste S.p.A., Italy) to between 6.0 and 8.0 m below ground surface. Sub-samples collected at 0.5 m depth intervals from each location were immediately transferred to PE bottles and frozen until analysis. Elemental and mineralogical analyses were previously conducted on bulk coke core samples to delineate bulk elemental relationships.[16] Thin sections were prepared for select coke samples to facilitate spectroscopic analyses. These samples were freeze-dried, vacuum-embedded in medical-grade epoxy, and mounted on 27 by 47 mm quartz-glass slides using cyanoacrylate adhesive. The sections were then ground and polished to 30 μm thick using 0.5 μm diamond and synthetic kerosene to avoid dissolution of water-soluble phases.

Electron Micro-Analyses. Samples were examined using an electron microprobe analyzer (EMPA; JXA-8600 Superprobe, JEOL, Japan) fitted with an electron dispersive X-ray (EDX) detector. A 20 nm thick C coating was applied to thin sections before EMPA examination using a 15 kV acceleration voltage.

Synchrotron Micro-Analyses. Thin sections were examined by μXRF and μXANES spectroscopy on beamline 13-ID-E at the Advanced Photon Source, Argonne National Laboratory. The storage ring was operated at 102 mA current in continuous top-up mode during data collection. Incident beam energy was selected using a cryo-cooled double crystal monochromator fitted with Si(111) crystals. The incident beam was focused to a 2 by 2 μm spot size on mounted thin sections.

Two-dimensional μXRF mapping of the V Kα emission line was performed at incident energies of 5486 eV, 5492 eV, and 5600 eV to examine V distribution and speciation within coke particles. These energies were selected based upon preliminary V K-edge μXANES measurements. Fluorescence data was collected with a four-element Si drift detector (Vortex ME4, Hitachi, Japan) in continuous scanning mode using a 25 ms practical pixel time. Beamline software (GSECARS X-ray Microprobe Map Viewer, Version 8) and custom matrix manipulation code (MATLAB 2010a, MathWorks, USA) were used for XRF data processing, which included subtraction of the Ti Kβ signal from V Kα maps.

Subsequent locations for V K-edge μXANES measurements were identified from the μXRF maps. These measurements involved scanning the incident energy from -100 to +644 eV relative to the theoretical V (5465 eV) K-edge. The energy resolution was 0.1 eV across the absorption edge. Sample spectra were collected in fluorescence mode using the same Si drift detector, while reference spectra were collected in transmission mode. Reference materials were prepared by grinding, diluting in BN, and packing into 0.5 mm thick polytetrafluoroethylene holders between two layers of polyimide adhesive tape. The Athena module of the Demeter software package (Version 0.9.21)[34] was used for data reduction and analysis. Linear combination fitting (LCF) was performed from −30 to +65 eV relative to the theoretical V

(5465 eV) K-edge. Reference spectra for V(V) oxide [V_2O_5], V(IV) octaethyl porphyrin (VOOEP), V(IV) tetraphenyl porphyrin (VOTPP), V(IV) bis-phenyl butane dionate (VOPBD), and roscoelite [$K(Al,V)_3Si_3O_{10}(OH)_2$][35] , and vanadium carbide [VC] were measured and considered during LCF analysis.

The V Kα μXRF mapping at 5486 and 5492 eV was performed to further assess the spatial distribution of V(IV) and V(III) within coke particles. These energies were selected because they corresponded to maximum absorbance of the roscoelite white line (5486 eV) – surrogate for octahedrally-coordinated V(III) – and the maximum absorbance of the VOOEP edge (5492 eV). Additionally, these energies avoided issues with potential contributions from V(V) to the V(IV) pre-edge peak. Speciation maps were generated by dividing the Ti Kβ-subtracted and I_0-normalized V Kα μXRF map obtained at an incident energy of 5486 eV, by those obtained at an incident energy of 5492 eV. The resulting quotient maps provide spatial information on the relative distribution of V(IV) porphyrin complexes and octahedrally-coordinated V(III) as V Kα counts per second ratios.

RESULTS AND DISCUSSION

Pore-water geochemistry. Geochemical conditions within the CB and CW deposits were characterized by a shallow mixing zone between meteoric water and OSPW isotopic signatures. This mixing zone was delineated from pore-water $\delta^{18}O$ values and Cl concentrations, which were strongly correlated (R = 0.77) and exhibited distinct depth-dependent trends (Figure 2). More depleted $\delta^{18}O$ values characteristic of meteoric water[36] were generally observed in shallow wells. Pore-water Cl concentrations ranged from 0 to 200 mg L^{-1} in these shallow wells and increased to greater than 400 mg L^{-1} with depth. Less depleted $\delta^{18}O$ and higher Cl

concentrations are consistent with OSPW[36], which was predominant in deeper wells at most locations. Similar to Cl, DOC concentrations generally increased with depth below the water table; however, with the exception of samples from location C, concentrations were consistently below 8 mg L^{-1}. This mixing zone was, however, less pronounced at location CB where Cl concentrations remained low to 8 m depth. Although the mixing zone depth varied among the remaining locations, the transition from low to elevated Cl concentrations was typically positioned between 2 and 4 m below the water table.

Pore-water pH ranged from 6.2 to 8.4 and generally increased with depth below the water table. Redox potential (Eh) decreased concomitantly with depth from between 300 and 550 mV to less than 100 mV at several locations (i.e., AB, AM, AX). The largest pH and Eh variations were observed within 2 m of the water table, which ranged from 0.6 to 4.5 m below ground surface among all locations. These variations, therefore, occurred above the upper boundary of the mixing zone between mildly acidic meteoric water with underlying OSPW, which is characterized by alkaline pH and anoxic conditions.[29]

Pore-water vanadium. Dissolved V concentrations were commonly elevated immediately below the water table and decreased rapidly with depth at all locations (Figures 2, 3). Vanadium concentrations ranged from less than 0.01 to 3.0 mg L^{-1}; however, values were consistently less than 0.5 mg L^{-1} at depths greater than 1.5 m below the water table. These rapid declines in pore-water V generally correspond to the zone of increasing pH and decreasing Eh.

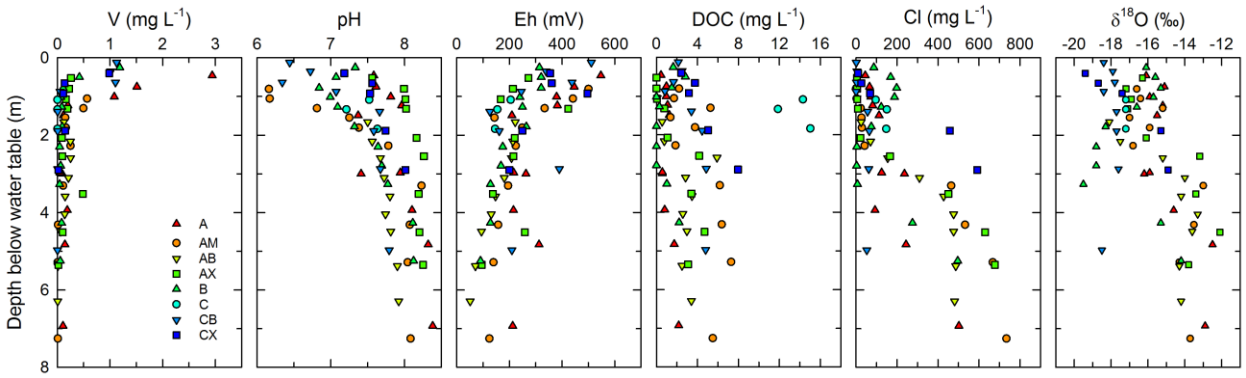

Figure 2. Depth profiles of pore-water V, pH, Eh, $\delta^{18}O$ and Cl for all sites relative to water table elevation.

Vanadium concentrations were significantly ($p < 0.05$) correlated with Eh values (R = 0.65) and thermodynamic modelling indicated $H_2VO_4^-$ was consistently the dominant aqueous species. These findings are consistent with previous research[21] that showed V(V) oxyanions exhibit greater mobility in natural waters. Although dissolved V(IV) and V(V) species have been detected in pore water of a covered oil sands petroleum coke deposit,[26] subsequent oxidation of V(IV) to V(V) is likely under oxic conditions.[27] Oxygen ingress into the uncovered CB deposit was expected given the high permeability of coke deposits.[37] Therefore, oxidation is likely to occur during V release and transport as infiltrating meteoric water migrates downward through the vadose zone. Elevated Eh values and V concentrations near the water table, therefore, suggest oxic conditions dominated within the vadose zone of the CB and CW deposits.

Depth profiles of Fe, Mn, SO_4 and H_2S were generally consistent among Sites A and AM (Figure 3), which exhibited distinct differences in dissolved V concentrations. Dissolved Fe and Mn concentrations exhibited maximum concentrations of 0.2 and 0.6 mg L^{-1} near the upper boundary of the mixing zone between meteoric water and OSPW. Elevated V concentrations typically corresponded to low Fe concentrations observed above this zone (Figures S1, S1). Thermodynamic modelling indicated that Mn(II) dominated Mn speciation and predicted the

presence of both Fe(II) and Fe(III). However, poor agreement between measured and theoretical Eh values is well established[38] and slight decreases (i.e., -50 mV) in input Eh values shifted model predictions to Fe(II) as the dominant Fe oxidation state. Dissolved H_2S concentrations approached 10 μg L^{-1} proximal to maximum Fe and Mn concentrations, suggesting a sharp transition from oxic to anoxic conditions at the upper boundary of the mixing zone between meteoric water and OSPW. The concentration of DOC increased downward slightly, corresponding to a transition to OSPW and anoxic conditions, but exceeded 8 mg L^{-1} only at location C in the CW deposit. Reduction of V(V) can be coupled with microbial oxidation of organic matter;[39] however, rates generally decrease with increasing pH and are slowest above pH 6.[24] Reduction of V(IV) to V(III) coupled with H_2S oxidation is possible; however, reduction rates are slow even at H_2S concentrations much higher than those measured.[40] Therefore, the occurrence of elevated V concentrations under anoxic conditions suggests that V(V) reduction was inhibited. Complexation of V(IV) or V(III) with organic and inorganic ligands has potential to inhibit redox transformations and enhance solubility.[24,27,40] Nevertheless, V concentrations within and below the mixing zone consistently decreased to less than 0.2 mg L^{-1} with depth at all locations including Sites A and AM.

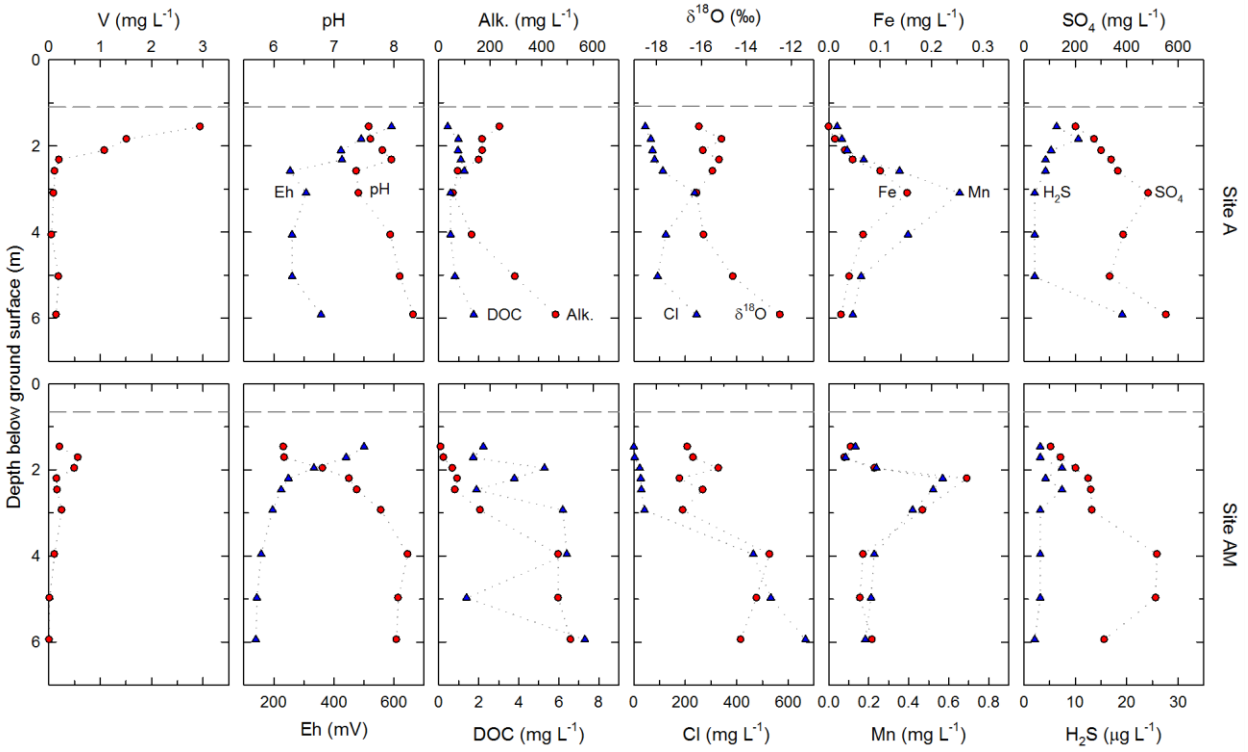

Figure 3. Depth profiles of pore-water V, pH, Eh, alkalinity (Alk.; as $CaCO_3$), Cl, Fe, Mn, SO_4, and H_2S at Sites A and AM. Horizontal dashed line represents the water table elevation at the time of sampling.

Previous laboratory studies have reported V concentrations in coke leachates generally increase with pH.[5,21,25,41] Although site-dependent variations in redox conditions were not apparent, shallow wells at Sites A and AM exhibited substantial differences in pH and alkalinity. Dissolved V concentrations ranged from 1.0 to 3.0 mg L^{-1} within the upper 2 m of the saturated zone at Site A (Figure 3). Pore-water pH at this site was consistently greater than 7.4 which is higher than the point of zero charge (pH_{PZC}) of 6.5 ± 0.3 of oil sands fluid petroleum coke.[41] In contrast, pore-water pH increased from 6.1 to 8.1 with depth at Site AM, where the maximum V concentration was 0.6 mg L^{-1}. Thermodynamic modelling indicated that pore-water was consistently undersaturated with respect to calcium vanadates and other V(V) phases. These site-dependent differences in V concentrations could, therefore, result from pH-dependent sorption of V(V) oxyanions onto coke particle surfaces. Coke particles would exhibit net positive surface

charge within the upper 2 m of the saturated zone at Site AM. Sorption of $H_2VO_4^-$ onto coke particle surfaces would limit dissolved V concentrations at this site. Less extensive $H_2VO_4^-$ sorption at higher pH could explain higher V concentrations observed at Site A. Previously-reported positive relationship between dissolved V and HCO_3^- concentrations in coke leachates[6] may result from formation of neutral or negatively-charged aqueous V(IV) carbonate complexes (e.g., $VOCO_3^0$, $VO(OH)CO_3^-$).[24,40] Although alkalinity was greater than 100 mg L^{-1} (as $CaCO_3$) for Site A samples that exhibited V concentrations above 1 mg L^{-1}, modelling suggests that formation of aqueous V(IV) species was thermodynamically unfavorable.

Solid-Phase Geochemistry. Fluid petroleum coke particles were composed of a sub-spherical core bounded by several successive concentric layers (Figure S3). These concentric layers were comprised of two zones: (1) an inner region measuring 5 to 10 μm thick; and (2) an outer margin measuring 1 to 5 μm thick. The inner region of individual layers was comprised mostly of C and S and generally consistent with bulk coke composition.[15] In contrast, the outer margins contained elevated K, Al, Si, Ca and Mg contents relative to C and S, and both Fe and Ti were commonly detected (Figure S4). Previous TEM-EDX analysis of oil sands fluid petroleum coke identified V-bearing nanocrystalline mineral clusters containing Si, O, S and Fe. However, these samples were crushed prior to analysis and the location of these clusters within coke particles was not reported.[12] The chemical and mineralogical composition of coke is derived from the bitumen source; therefore, spatial variations are attributed to the fluid coking process. Coke particles are continuously circulated between burner vessel – operated at 480 to 565°C – and coker vessel (i.e., fluidized bed reactor).[42] Bitumen is sprayed onto hot coke particles within the coker vessel to facilitate thermal decomposition of the non-distillable

bitumen fraction. Volatile compounds are recovered and residual hydrocarbons form a new layer at particle surfaces.

Vanadium Speciation in Coke Particles. Coke particles exhibited heterogeneous V distribution with concentrations typically highest at the outer margins of concentric layers (Figure 4). Additionally, V K-edge μXANES spectra commonly differed between the inner region and outer margin of individual concentric layers (Figure 4, Table S1). Spectra obtained from layer inner regions were generally consistent with bulk V K-edge spectra for oil sands fluid petroleum coke.[16] These spectra exhibited a distinct pre-edge peak positioned at 5469 eV, which may be associated with the V(IV) or V(V) oxidation state. However, LCF analysis of these μXANES spectra and previous finite difference modelling of the near-edge structure (FDMNES)[16,43] indicated that V(IV) in porphyrin-like square-pyramidal N and O coordination dominated V speciation (Table S1). Nevertheless, V(V) likely constituted minor to trace component of these V K-edge μXANES spectra that was not associated with V(IV) porphyrin complexes.

Corresponding μXANES spectra obtained from outer margins of individual concentric layers exhibited a lower magnitude pre-edge peak at 5469 eV. Additionally, these spectra exhibited a doublet feature between 5484 and 5499 eV that was inconsistent with V K-edge spectra for V(IV) porphyrins.[44] These spectral features were, however, generally consistent with V(III) substituted into distorted octahedral O-coordinated sites in (phyllo)silicate minerals.[35,45] The phyllosilicate roscoelite [$KAlV_2Si_3O_{10}(OH)_2$], which contains this manner of V(III) coordination, exhibited V K-edge XANES spectra[35] similar to those obtained from outer margins. Similar distorted octahedrally-coordinated V(III) has previously been reported for

coals.[45] Similar to the layer inner regions, V(V) likely represented a minor to trace component of sample spectra from the our margins of concentric layers.

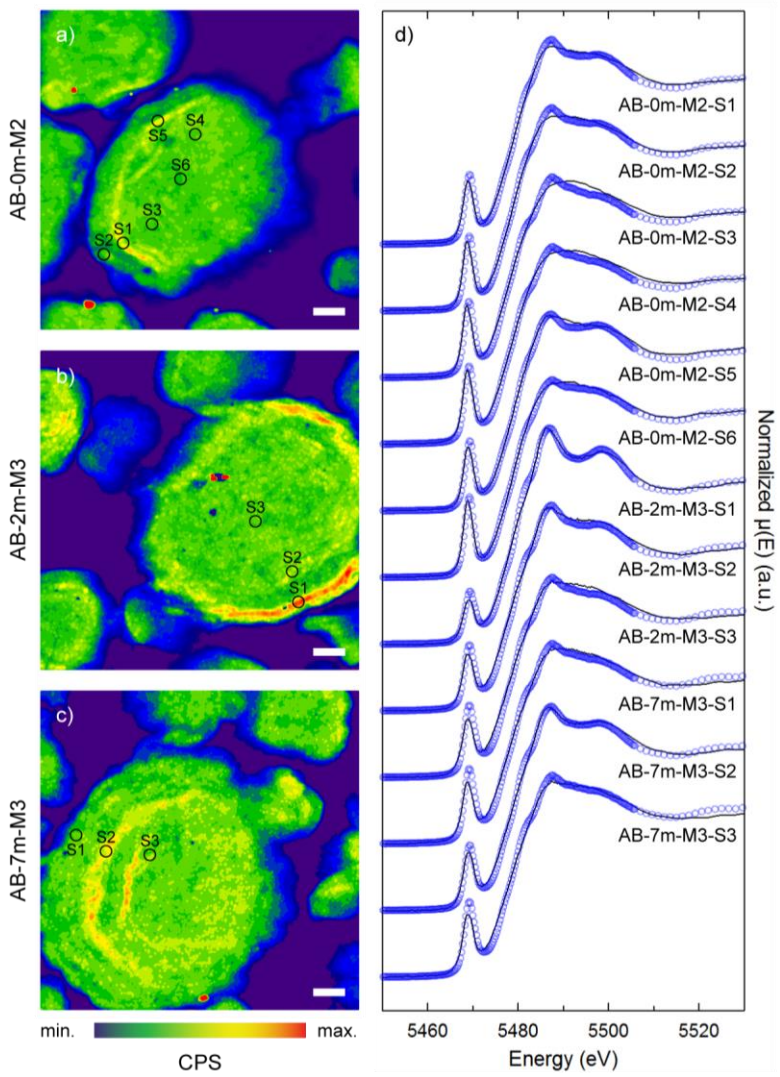

Figure 4. Vanadium Kα μXRF maps obtained at 5600 eV for samples from depths of 0 m (a), 2 m (b) and 7 m (c) for location AB in the CB deposit. (d) Measured (solid lines) and fitted (open circles) V K-edge μXANES spectra for multiple spots from V Kα maps. Scale bars on μXRF maps represent 20 μm and units are counts per second (CPS).

Linear combination fitting was performed for V K-edge μXANES spectra (n = 34) from selected spots on multiple V Kα μXRF maps (n = 8) for various sampling locations. The LCF results revealed that relative proportions of V(IV) porphyrins compared to octahedrally-

coordinated V(III) ranged from 5.8 to 0.8 (Table S1). Fitted spectra for particle cores and layer inner regions comprised up to 86% V(IV) porphyrin reference spectra (i.e., VOOEP, VOPBD) (Figure S5). In contrast, fitted spectra for outer layer margins included up to 50% octahedrally-coordinated V(III) standard (i.e., roscoelite). For example, LCF results for a sample obtained 2.0 m below surface at site AB (AB-2m) displayed substantial spatial differences (Figure 4). Approximately 50% of a μXANES spectrum from the outer layer margin of this sample (AB-2m-M3-S1) was attributed to distorted octahedrally-coordinated V(III). Vanadium(IV) porphyrin reference spectra accounted for greater than 60% of spectra obtained for other spots (AB-2m-M3-S2, AB-2m-M3-S3) on this sample, which were located within a layer inner region and particle core, respectively. These results revealed that V(IV) porphyrins dominated V speciation within coke particles; however, octahedrally-coordinated V(III) was prevalent at the outer margins of concentric rings. Vanadium(V) phases exhibit a high-intensity pre-edge peak shifted to slightly higher energy compared to V(IV) porphyrins (Figure S5). The V(V) spectrum slightly improved fits over the pre-edge peak region (5465 to 5473 eV), suggesting the presence of a minor to trace V(V) component.

Similar spatial variations in the relative proportion of V(IV)-porphyrin complexes and octahedrally-coordinated V(III) were revealed by speciation mapping (Figure 5). These maps showed that V(IV)-porphyrin complexes generally dominated solid-phase V speciation. However, octahedrally-coordinated V(III) was commonly more abundant in outer margins of layers (i.e., AB-7m-M4-S3), where total V Kα counts were generally highest, compared to inner regions of layers (i.e., AB-7m-M4-S1, AB-7m-M4-S2). These maps provided speciation information at a much higher spatial coverage compared to V K-edge μXANES point

measurements. Nevertheless, interpretations based on these speciation maps were consistent with the µXANES data.

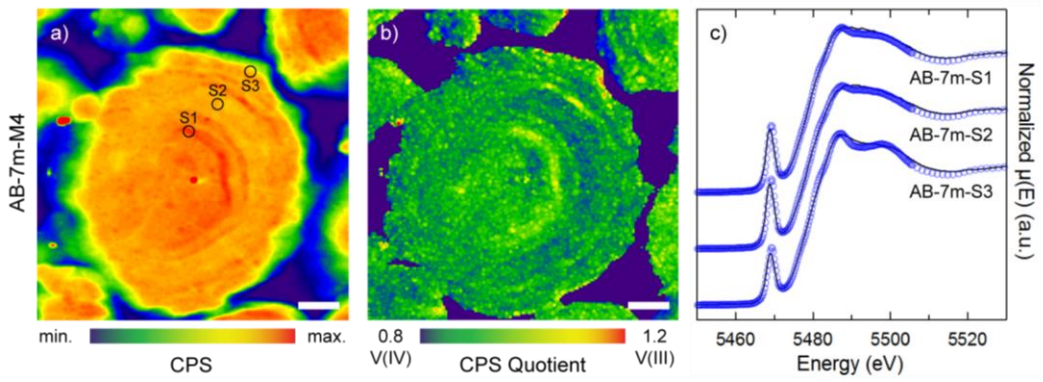

Figure 5. (a) Vanadium Kα µXRF map obtained at incident energy of 5600 eV for sample from depth of 7 m at location AB in the CB deposit. (b) Corresponding oxidation state map calculated from the pixel-wise quotient of V Kα µXRF maps obtained at incident energies of 5486 and 5492 eV. (c) Measured (solid lines) and fitted (open circles) V K-edge µXANES spectra for selected spots on this sample. Scale bars on µXRF maps represent 20 µm and units are counts per second (CPS) and CPS quotient.

Conceptual Model of V Mobility. Oil sands fluid petroleum coke particles exhibit systematic zonation of V species, which is attributed to the coking process. Although bulk V speciation is dominated by V(IV) porphyrin complexes,[16] octahedrally-coordinated V(III) was abundant at outer margins of concentric layers. The prevalence of V(III) at coke-particle surfaces – the outer margin of outer-most concentric layer – and expected stability of V(IV) porphyrin complexes suggest V(III) is a potential dissolved V source. However, the minor to trace V(V) component represents another possible contributor to dissolved V in fluid petroleum coke deposits.

Thermodynamic modeling indicated that the V(V) oxyanion $H_2VO_4^-$ dominated aqueous speciation and consistent undersaturation of pore-water with respect to V(V) phases (e.g., Ca-vanadates). Extensive V leaching in the presence of deionized water and exchangeable ions has

previously been reported for fluid petroleum coke.[16] Therefore, extensive V(V) accumulation within coke particles is unlikely. These results suggest that oxidative V(III) weathering at coke particle surfaces may produce a pool of soluble V(V) within the vadose zone, which could be transported downward to the saturated zone with infiltrating meteoric water. However, the presence of an initial V(V) pool produced during coking cannot be ruled out.

Dissolved V concentrations within the saturated zone were strongly controlled by pH and redox conditions. The highest V concentrations were generally observed under oxic conditions and neutral to alkaline pH. Substantial decreases in dissolved V concentrations were, however, observed for the same pH conditions under anoxic conditions. Since precipitation of V(V) phases was thermodynamically unfavorable, these observations suggest that V(V) reduction to V(IV) or V(III) may lead to sorption of cationic species at alkaline pH or to precipitation of secondary (hydr)oxide phases. Overall, these results indicate that V leaching and mobility are enhanced when fluid petroleum coke is exposed to oxygen in the presence of meteoric waters.

ASSOCIATED CONTENT

Supporting Information

One additional table and five additional figures referenced in the text (PDF).

AUTHOR INFORMATION

Corresponding author

*E-mail: matt.lindsay@usask.ca; phone: 306-966-5693; fax: 306-966-8593

Notes

The authors declare no competing financial interest.

ACKNOWLEDGEMENTS

Funding was provided by the Natural Sciences and Engineering Council of Canada (NSERC) and Syncrude Canada Ltd. through the NSERC Industrial Research Chairs program (Grant No. IRCPJ-450684-13). A portion of the research described in this paper was performed at the Advanced Photon Source, a U.S. Department of Energy (DOE) Office of Science User Facility operated for the DOE Office of Science by Argonne National Laboratory under Contract No. DE-AC02-06CH11357. We thank N. Chen, T. Lanzirotti and M. Newville for assistance with XAS data collection and analysis.

REFERENCES

(1) Furimsky, E. Gasification of oil sand coke: Review. *Fuel Proc. Technol*. **1998**, *56* (3), 263–290. DOI 10.1016/S0378-3820(98)00048-4

(2) *ST98-2015: Alberta's Energy Reserves 2014 and Supply/Demand Outlook 2015–2024*. Alberta Energy Regulator: Calgary, AB, 2015; https://www.aer.ca/documents/sts/ST98/ST98-2015.pdf

(3) Fedorak, P.M; Coy, D.L. Oil sands cokes affect microbial activities. *Fuel* **2006**, *85*, 1642-1651. DOI 10.1016/j.fuel.2006.02.015

(4) Puttaswamy, N.; Turcotte, D.; Liber, K. Variation in toxicity response of *Ceriodaphnia dubia* to Athabasca oil sands coke leachates. *Chemosphere* **2010**, *80* (5), 489–497. DOI 10.1016/j.chemosphere.2010.04.071

(5) Puttaswamy, N.; Liber, K. Identifying the causes of oil sands coke leachate toxicity to aquatic invertebrates. *Environ. Toxicol. Chem.* **2011**, *30* (11), 2576-2585. DOI 10.1002/etc.653

(6) Puttaswamy, N.; Liber, K. Influence of inorganic anions on metals release from oil sands coke and on toxicity of nickel and vanadium to Ceriodaphnia dubia. *Chemosphere* **2012**, *86*, 521-529. DOI 10.1016/j.chemosphere.2011.10.018

(7) Nakata, C.; Qualizza, C.; MacKinnon, M.D.; Renault, S. Growth and physiological responses of *Triticum aestivum* and *Deschampsia caespitosa* exposed to petroleum coke. *Water, Air, Soil, Pollut.* **2011**, *216* (1), 59-72. DOI 10.1007/s11270-010-0514-x

(8) Baker, L.F., Ciborowski, J.J.H., MacKinnon, M.D. Petroleum coke and soft tailings sediment in constructed wetlands may contribute to the uptake of trace metals by algae and aquatic invertebrates. *Sci. Total Environ*. **2012**, *414*, 177-186. DOI 10.1016/j.scitotenv.2011.10.011

(9) Zhang, Y.; Shotyk, W.; Zaccone, C.; Noernberg, T.; Pelletier, R.; Bicalho, B.; Froese, D.G.; Davies, L.; Martin, J. Airborne petcoke dust is a major source of polycyclic aromatic hydrocarbons in the Athabasca oil sands region. *Environ. Sci. Technol.* **2016**, *50* (4), 1711-1720. DOI 10.1021/acs.est.5b05092

(10) Caruso, J.A.; Zhang, K.; Schroeck, N.J.; McCoy, B.; McElmurry, S.P. Petroleum coke in the urban environment: A review of potential health effects. *Int. J. Environ. Res. Public Health* **2015**, *12* (6), 6218–6231. DOI 10.3390/ijerph120606218

(11) Dechaine, G.P.; Gray, M.R. Chemistry and association of vanadium compounds in heavy oil and bitumen and implications for their selective removal. *Energy Fuels* **2010**, *24*, 2795-2808. DOI 10.1021/ef100173j

(12) Zuliani, J.E.; Miyata, T.; Mizoguchi, T.; Feng, J.; Kirk, D.W.; Jia, C.Q. Characterization of vanadium in oil sands fluid petroleum coke using electron microscopy. *Fuel* **2016**, *178*, 124–128. DOI 10.1016/j.fuel.2016.03.015

(13) Har, S. Characterization of Oil Sands Fluid Coke. M.Sc. Thesis, University of Alberta, Edmonton, AB, 1981.

(14) Chung, K.H.; Janke, L.C.G.; Dureau, R.; Furimsky, E. Leachability of cokes from Syncrude stockpiles. *Environ. Sci. Eng.* **1996**, *9* (1), 50-53.

(15) Zubot, W.; MacKinnon, M.D.; Chelme-Ayala, P.; Smith, D.W.; Gamal El-Din, M. Petroleum coke adsorption as a water management option for oil sands process-affected water. *Sci. Total Environ.* **2012**, *427-428*, 364-372. DOI 10.1016/j.scitotenv.2012.04.024

(16) Nesbitt, J.A.; Lindsay, M.B.J.; Chen, N. Geochemical characteristics of oil sands fluid petroleum coke. *Appl. Geochem.* **2017**, *76*, 148-158. DOI 10.1016/j.apgeochem.2016.11.023

(17) Reynolds, J.G.; Gallegos, E.J.; Fish, R.H; Komlenic, J.J. Characterization of the binding sites of vanadium compounds in heavy crude petroleum extracts by electron paramagnetic resonance spectroscopy. *Energy Fuels* **1987**, *64* (1), 36-44. DOI 10.1021/ef00001a007

(18) Filby, R.H.; Strong, D. Nickel (II) and vanadium (IV) complexes in Alberta oil-sand bitumens. Tar sand and oil upgrading technology. *AIChE Symp. Ser.* **1991**, 282.

(19) Grosjean, E.; Adam, P.; Connan, J.; Albrecht, P. Effects of weathering on nickel and vanadyl porphyrins of a Lower Toarcian shale of the Paris basin. *Geochim. Cosmochim. Acta* **2004**, *64* (4), 789–804. DOI 10.1016/S0016-7037(03)00496-4

(20) Furimsky, E. Characterization of cokes from fluid/flexi-coking of heavy feeds. *Fuel Process. Technol.* **2000**, *67*, 205-230. DOI 10.1016/S0378-3820(00)00103-X

(21) Wehrli, B.; Stumm, W. Vanadyl in natural waters: Adsorption and hydrolysis promote oxygenation. *Geochim. Cosmochim. Acta* **1989**, *53*, 69-77. DOI 10.1013/0016-7037(89)90273-1

(22) Peacock, C.L.; Sherman, D.M. Vanadium(V) adsorption onto goethite (α-FeOOH) at pH 1.5 to 12: a surface complexation model based on ab initio molecular geometries and EXAFS

spectroscopy. *Geochim. Cosmochim. Acta* **2004**, *68* (8), 1723–1733. DOI 10.1016/j.gca.2003.10.018

(23) Wright, M.T.; Stollenwerk, K.G.; Belitz, K. Assessing the solubility controls on vanadium in groundwater, northeastern San Joaquin Valley, CA. *Appl. Geochem.* **2014**, *48*, 41–52. DOI 10.1016/j.apgeochem.2014.06.025

(24) Huang, J.-H.; Huang, F.; Evans, L.; Glasauer, S. Vanadium: Global (bio)geochemistry. *Chem. Geol.* **2015**, *417*, 68–89. DOI 10.1016/j.chemgeo.2015.09.019

(25) Zubot, W. Removal of naphthenic acids from oil sands process water using petroleum coke. M.Sc. Eng. Thesis, University of Alberta, Edmonton, AB, 2010.

(26) Baes, C.F., Mesmer, R.E. *The hydrolysis of cations*. John Wiley & Sons, 1976.

(27) Jensen-Fontaine, M. Vanadium speciation in samples relevant to the Athabasca oil sands region. M.Sc. Thesis, University of Alberta, Edmonton, AB, 2012.

(28) Li, X.S.; Glasauer, S.; Le, X.C. Erratum to "Speciation of vanadium in oilsand coke and bacterial culture by high performance liquid chromatography inductively coupled plasma mass spectrometry" [Anal. Chim. Acta 602 (2007) 17-22] (DOI:10.1016/j.aca.2007.09.004). *Anal. Chim. Acta* **2009**, *648* (1), 128. DOI 10.1016/j.aca.2009.06.053

(29) Allen, E.W. Process water treatment in Canada's oil sands industry: I. Target pollutants and treatment objectives. *J. Environ. Eng. Sci.* **2008**, *7* (2), 123–138. DOI 10.1139/S07-038

(30) Nordstrom, D.K. Thermochemical redox equilibria of ZoBell's solution. *Geochim. Cosmochim. Acta* **1977**, *41*, 1835-1841. DOI 10.1016/0016-7037(77)90215-0

(31) Light, T.S. Standard solution for redox potential measurements. *Anal. Chem.* **1972**, *44* (6), 1038-1039. DOI 10.1021/ac60314a021

(32) Wassenaar, L.I.; Hendry, M.J.; Chostner, V.L.; Lis, G.P. High resolution pore water δ^2H and $\delta^{18}O$ measurements by H_2O(liquid)-H_2O(vapor) equilibration laser spectroscopy. *Environ. Sci. Technol.* **2008**, *42*, 9262-9267. DOI 10.1021/es802065s

(33) Parkhurst, D.L.; Appelo, C.A.J. Description of input and Examples for PHREEQC - A computer program for speciation, batch-reaction, one-dimensional transport, and inverse geochemical calculations. In *U.S. Geological Survey Techniques and Methods, Book 6*; USGS 2013; p 497.

(34) Ravel, B.; Newville, M. ATHENA, ARTEMIS, HEPHAESTUS: data analysis for X-ray absorption spectroscopy using IFEFFIT. *J. Synchrotron Radiat.* **2005**, *12*, 537-541. DOI 10.1107/S0909049505012719

(35) Wong, J.; Lytle, F.W.; Messmer, R.P.; Maylotte, D.H. K-edge absorption spectra of selected vanadium compounds. *Phys. Rev. B* **1984**, *30* (10), 5596-5610. DOI 10.1103/PhysRevB.30.5596

(36) Baer, T.J. An evaluation of the use of natural stable isotopes of water to track water movement through oil sands mine closure landforms. M.Sc. Thesis, University of Saskatchewan, Saskatoon, SK, 2014. (37) Lahmira, B.; Barbour, L.; Huang, M. Numerical modeling of gas flow in the Suncor coke stockpile covers. *Vadose Zone J*. **2013**, *13* (1), 1-12. DOI 10.2136/vzj2013.07.0119

(38) Lindberg, R.D.; Runnells, D.D. Ground Water Redox Reactions: An Analysis of Equilibrium State Applied to Eh Measurements and Geochemical Modelling. *Science* **1984**, *225* (4665), 925-927. DOI 10.1126/science.225.4665.925

(39) Borch, T.; Kretzschmar, R.; Kappler, A.; Van Cappellen, P.; Ginder-Vogel, M.; Voegelin, A.; Campbell, K. Biogeochemical Redox Processes and their Impact on Contaminant Dynamics. *Environ. Sci. Technol.* **2010**, *44*, 15-23. DOI 10.1021/es9026248

(40) Wanty, R.B.; Goldhaber, M.B. Thermodynamics and kinetics of reactions involving vanadium in natural systems: Accumulation of vanadium in sedimentary rocks. *Geochim. Cosmochim. Acta* **1992**, *56* (4), 1471–1483. DOI 10.1016/0016-7037(92)90217-7 10.1016/j.gca.2003.10.018

(41) Pourrezaei, P.; Alpatova, A.; Chelme-Ayala, P.; Perez-Estrada, L.A.; Jensen-Fontaine, M.; Le, X.C.; Gamal el-Din, M. Impact of petroleum coke characteristics on the adsorption of the organic fractions from oil sands process-affected water. *Int. J. Environ. Sci. Technol.* **2014**, *11*, 2037-2050. DOI 10.1007/s13762-013-0406-x

(42) Anthony, E. Fluidized bed combustion of alternate solid fuels; status, success and problem of the technology. *Prog. Energy Combust. Sci.* **1995**, *21*, 239-268. DOI 10.1016/0360-1285(95)00005-3

(43) Bunău, O.; Joly, Y. Self-consistent aspects of x-ray absorption calculations. *J. Phys.: Condens. Matter* **2009**, *21*, 345501 (11pp). DOI 10.1088/0953-8984/21/34/345501

(44) Lytle, F. Cold Lake asphaltene V and Ni XAS spectra. International X-ray Absorption Society XAFS Database, 1983. Retrieved from http://ixs.iit.edu/database/data/Farrel_Lytle_data/RAW/ on Mar. 31, 2016.

(45) Maylotte, D.H.; Wong, J.; St. Peters, R.L.; Lytle, F.W; Greegor, R.B. X-ray absorption spectroscopic investigation of trace vanadium sites in coal. *Science* **1981**, *214* (4520), 554-556. DOI 10.1126/science.214.4520.554